STRESS AND STRAIN DISTRIBUTION AROUND CRACKS IN COMPLEX PRESSURE VESSEL CONFIGURATIONS

C. RUIZ,

Department of Engineering Science,
University of Oxford, Oxford, United Kingdom

ABSTRACT

The specific problem discussed in this paper consists in the determination of the stress distribution around cracks in the immediate vicinity of nozzle-to-shell junctions. A technique is described for the measurement of the stress intensification factor, based on the use of a photoelastic layer sandwiched within an optically inert model. The relevance of the value thus found for the characterisation of the severity of the crack is finally discussed.

1. Introduction

One of the problems that designers and inspectors have to face in the pressure vessel field is the assessment of the severity of defects, and in particular surface cracks, situated in regions of complex geometry. Most of the work done at present is limited to the determination of the disturbance created by cracks in relatively simple configurations under virtually uniform loading conditions, e.g., plates loaded in their plane, through slits in cylindrical vessels remote from all other discontinuities and part-through notches in vessels. Analytical, numerical and experimental techniques have all been used. It is, however, clear that the results thus achieved can only be applied to the configurations for which they were arrived. It is also abundantly clear that the failure of pressure vessels, fabricated to meet any of the generally accepted standards is usually initiated by defects which are situated in the vicinity of a large structural discontinuity such as at the junction of a nozzle to a cylindrical barrel. Present methods fail to provide a clear indication of how the available results can be applied to such a complex geometry. It is the purpose of this paper to suggest how this can be done, if not in an exact, at least in an approximate way, using an experimental technique previously developed [1, 2].

From a large number of fatigue tests of pressure vessel connections [3], it has been concluded that the two most common types of failure are initiated by cracks, opening up under the action of hoop stresses in the main shell. These cracks may be of two types:-

a) in flush nozzles of small bore relative to the main shell diameter, axial cracks at the crotch corner, starting from the inside wall surface.

b) in large bore openings, axial cracks at 90° to the crotch, starting from the outside wall surface.

This conclusion is consistent with the experimental stress analyses reported by the P.V.R.C. [4], while under static bursting most vessels would appear to fail due to cracks of

type (b) [5]. In this investigation it was therefore decided to concentrate in the determination of stresses and strains in cracks of type (b).

2. Description of models and experimental technique

The models used were similar to those described in a previous publication [2]. The material used for their manufacture was 'Perspex', modified by increasing the proportion of plasticiser to 10% to make it virtually non-birefringent under load. Stresses are measured photoelastically, by observing the fringes produced in an epoxy sheet embedded in the 'Perspex'. Contrary to the frozen stress technique, the model is not destroyed during test and may be modified and re-examined to determine the effect of a given change in its geometry over the stress system. The main dimensions of the models tested are shown in Fig. 1 and Table 1. Models 1 to 7 were similar to some of the models tested under the auspices of the PVRC [4] in order to compare the results from this method to those obtained by means of the more conventional frozen stress technique. Since the PVRC tests did not include the effect of cracks, this comparison is restricted to plain vessels, without any defects.

One difficulty associated with the interpretation of photoelastic results in models with very sharp stress raisers is the correct assessment of peak stress at the free surfaces. This is due to edge effects which, while minimised by the use of parallel light and long focal length photographic lenses interfere with the fringes in the immediate proximity of the stress raiser itself. In the present investigation the course followed was based on the definition of the stress intensification factor (s.i.f.). In the vicinity of a crack, i.e. within a distance from the crack tip equal to about the crack depth, the Westergaard stress function can be used to provide an approximation to the stress distribution. Measuring the stresses along a line perpendicular to the crack and tangential to the crack front, it can be shown that [2]

$$\sigma_1 - \sigma_2 = \frac{\text{s.i.f.}}{\sqrt{2r}} \qquad (1)$$

where $(\sigma_1 - \sigma_2)$ is the difference between the two principal stresses at a point distant r from the crack front (see Fig. 2). It must be emphasised that equation 1 fails to give an accurate description of the state of stress at a point remote from the crack tip, since when r tends to infinity $(\sigma_1 - \sigma_2)$ must tend towards the value of the nominal hoop shell stress, σ_θ and not to zero as implied by the equation. On the other hand, immediately next to the crack tip itself, Westergaard stress function ceases to be applicable. The stress distribution is there dependent on the actual crack profile, modified by small plastic deformation under load. The main advantage of using eq. (1), in spite of its limitations, is to provide results consistent with the basic principles of linear elastic fracture mechanics. To this end, eq. (1) is expressed in non-dimensional form.

$$\frac{\sigma_1 - \sigma_2}{\sigma} = \frac{\text{s.i.f.}}{\sigma\sqrt{2r}} = k\sqrt{\frac{a}{2r}} \qquad (2)$$

where $k = (\text{s.i.f.}) \quad \frac{1}{\sigma\sqrt{a}}$ is a geometrical dimensionless parameter. It will be noted that the stress intensity K_I is defined as,

$$K_I = k\sigma\sqrt{\pi a} \qquad (3)$$

The value of k for different configurations can be determined by measuring the slope of

the straight part of curves giving the variation of $(\sigma_1 - \sigma_2)/\sigma$ against $\sqrt{a/2r}$ as shown in Fig. 3. In that figure, the broken lines indicate the fact that eq. (2) ceases to be valid. This implies that the measured values of $(\sigma_1 - \sigma_2)/\sigma$ do not in fact lie along lines passing through the origin of co-ordinates but are slightly displaced as shown in the figure.

In the models, notches were machined by means of a milling cutter of 12 mm diameter, ground to a maximum thickness of 0.25 mm and to a smoothly tapering profile terminating in a sharp edge. Following a number of tests with plain cylindrical shells with longitudinal notches, it was found that the s.i.f. associated with this notch profile was no different from that previously found in notched and cracked vessels, a circumstance that can be explained by the tip blunting under load in the plastic. However, although the measured s.i.f. is less dependent on the notch or crack profile for such sharp stress raisers than it would be expected, the actual values of the peak stresses immediately next to the crack tip were higher than those near the notch in as much as it could be assessed by means of the photoelastic technique.

3. Characterisation of stress field

In the present investigation only the hoop stresses in the plane of the photoelastic layer, normal to the main shell generators, were determined. The effect of the opening, reinforced by the nozzle, is to introduce direct plus bending stresses, in such a way that, in the un-notched side of the model,

$$\sigma_d = \frac{\sigma_o + \sigma_i}{2} \qquad \sigma_b = \frac{\sigma_o - \sigma_i}{2} \qquad (4)$$

where σ_d is the direct stress at the shell/nozzle junction, σ_o and σ_i are respectively the peak stresses on the outside and inside surfaces and σ_b is the bending stress. The stress concentration factor (S.C.F.) is defined as the ratio between the maximum stress and the nominal shell hoop stress σ_n.

In the notched side of the model, the presence of the notch introduces a highly localised discontinuity whose effect is to increase the peak stress to an extremely high value. The severity of the notch is characterised by the value of k, determined as described in the previous section.

4. Test procedure and results

The models were supported on Vee blocks in a glass tank filled with medicinal paraffine to which was added bromo-naphthalene in order to match the refractive index of 'Perspex'. Loading was by means of a hand pump, using the same fluid that was used in the immersion tank. The model was observed in a conventional polariscope and the fringes photographed with a 36 inch focal length process lens. The position of the fringes was measured on the negative with an X-Y microscope.

The experimental values of the S.C.F. are shown in Fig. 4 against the parameter $\rho = (d/D)\sqrt{(D/T)}$. While there is considerable scatter, due to the different corner radii in otherwise identical models, it will be seen that all the experimental points are roughly along a straight line, showing the S.C.F. to be primarily a function of the parameter ρ. Good correlation was found between these results and those previously reported [4]. It is clear that higher S.C.F. might be obtained on longitudinal planes, but these were not de-

termined in the present series of tests. In all cases the maximum hoop stress was found to be σ_o, on the outside surface.

For the determination of the s.i.f. the stress variation along the hoop direction, as shown in Fig. 3, is plotted in Fig. 5, in which the stress at a given point is referred to the value of the peak stress σ_o. The slope of the straight part of the experimental curves represents the value of $\underline{k}$. With the exception of models 11 and 14, where values of $\underline{k}$ as low as about 0.45 were found, the values of k were found to vary between 0.55 and 0.70. Fig. 5 only reproduces stress values in the vicinity of the notch: the curves illustrated tend very rapidly towards $(\sigma_1 - \sigma_2)/\sigma_o = (1/S.C.F)$ as the ratio (r/a) increases above unity.

5. Interpretation of results

A method for the numerical determination of the s.i.f. associated with part-circular surface cracks in plates under plane loading has been described by Smith and Alavi [6]. While the method is only valid for semi-infinite solids, i.e. for those cases where the plate thickness is considerably larger than the crack depth, an approximate correction factor can be included to take into account the effect of the plate thickness. Using this technique, and evaluating the geometrical parameter $\underline{k}$ on the normal midplane to the crack, the results plotted in Fig. 6 are obtained. The numerical analysis can be extended to the case of bending by superimposing to the solution for simple tension the case of a linearly varying load normal to the crack plane. Due to the unavoidable inclusion of the thickness correction factor, some loss in accuracy will be experienced. In addition the stress gradient through the plate thickness results in a variation of the s.i.f. at a given position along the neck, with a maximum at the ends of the crack and a minimum at the centre. It may be postulated that the crack will open under the action of the s.i.f. integrated over the whole crack length, in which case the average s.i.f. will be a figure of merit representing the crack severity. On the other hand, the value of $\underline{k}$ that will be determined experimentally is averaged over the thickness of the photoelastic layer, and approximately equal to one half of the crack length. For very shallow cracks, with a half length-to-depth ratio considerably larger than unity the difference between experimental and averaged values of the s.i.f., assuming theory and experiment to be in agreement, is likely to be negligible, the difference between both values increasing as the crack becomes less shallow. The curves plotted in Fig. 7 represent the values of $\underline{k}$ for the plate in bending, averaged over the whole crack length. The curves for values of the crack depth-to-plate thickness ratio above 0.25 can only be considered to be approximative and are therefore shown in broken lines.

The stress variation through the shell thickness, assumed to be lineal, may be expressed as,

$$\frac{\sigma_1 - \sigma_2}{\sigma_o} = \left(\frac{\sigma_d}{\sigma_o}\right) + \left(\frac{\sigma_b}{\sigma_o}\right) \frac{2\zeta}{T} \qquad (5)$$

where σ_d and σ_b are as defined in eq. (4) and ζ is the distance to the shell mid surface. It is then possible to write,

$$k = \frac{\text{s.i.f.}}{\sigma_o \sqrt{a}} = \left(\frac{\sigma_d}{\sigma_o}\right) k_d + \left(\frac{\sigma_b}{\sigma_o}\right) k_b \qquad (6)$$

Equation 6 may be used to determine the effect that a crack will have on a given stress field, resulting from the combination of a direct and a bending stress. In the present tests

$$0.5 < \frac{\sigma_b}{\sigma_o} < 0.67$$

$$k_d = 0.9$$

$$k_b = 0.5$$

and it is found that $0.6 < k < 0.7$, a conclusion that agrees with the experimental results with the exception of models numbers 11 and 14. Considering that in both these models the ratio crack depth-to-shell thickness is as high as 0.63 this lack of agreement is not surprising given the approximative nature of the calculations.

6. Discussion

The correlation between experimental results and the predicted values from eq. (6) and Figs. 6 and 7 show a relative error of less than ± 15%, of the same order as the calculated or measured range. The narrow relative difference between the two extreme values of the geometrical parameter k, together with the fact that the notch shape was the same for all vessels entail a serious restriction to the general application of eq. (6), which can only be considered as providing a rough indication of k pending the results of further experiments.

The apparent insensitivity of the geometrical factor k to changes in the overall stress field and in the depth of the crack, relative to the shell thickness, is clear from the experiments and the calculation. It follows that the stress intensity factor is primarily dependent on the value of $(\sigma\sqrt{a})$, depending to a lesser degree on the actual stress distribution, within the range covered in these tests. Within the usual assumptions of linear elastic fracture mechanics, it is possible to interpret the s.i.f. as a measure of the severity of the crack, which is thus seen to depend on the product,

$$k\sigma_o\sqrt{a} = k(\sigma_{nominal} \times \text{S.C.F.})\sqrt{a} \qquad (7)$$

where k, equal to unity for an infinitely long crack of small depth compared to the plate thickness when the plate is under plane tension, is likely to be less than unity in all other practical cases.

Another conclusion that can be drawn from the above is that a reduction in defect size is not as effective in reducing its severity as a reduction in the stress level, i.e. in either the nominal stress or the S.C.F. That notch depth, crack length, or, in general, 'defect size' should have less influence than is generally supposed on the tendency to embrittlement has been advanced by Boyd amongst others [7]. This can be explained by considering the state of stress at the root of the notch, on its normal median plane. Given that Westergaard's function provides a sufficiently accurate representation for our purpose,

and applying von Mises' criterion, it can be shown that the yield locus is given by,

$$Y = \frac{\text{s.i.f.}}{\sqrt{2r}} \cos\frac{\upsilon}{2}\sqrt{(1 + 3\sin^2\frac{\upsilon}{2})} \qquad (8)$$

where Y is the uniaxial yield stress. This equation, valid for the plane stress case where

$\sigma_{axial} = 0$ takes the form,

$$Y = \frac{s.i.f.}{\sqrt{2r}} \cos\frac{\theta}{2}\sqrt{\left[(1-2\nu)^2 + 3\sin^2\frac{\theta}{2}\right]} \qquad (9)$$

for the plane strain case, where $\sigma_{axial} = \nu(\sigma_1 + \sigma_2)$. In both cases, ν is Poisson's ratio equal to about $\frac{1}{2}$ under conditions of unrestrained plastic flow. The yield loci, for $\nu = \frac{1}{2}$, are shown in Fig. 8.

From Fig. 8 it is quite obvious that identical values of the s.i.f., measured or calculated for a two dimensional stress or strain field, can give rise to entirely different plastic enclaves and thus to very different values of the plastic work required to open up a crack. To characterise the crack severity it then becomes essential to resort to a three dimensional stress or strain analysis, a difficult enough task in a simple problem such as a crack in a semi-infinite solid under uniform tension but quite daunting in any other practical situation. An alternative solution which is at present under consideration consists in the simultaneous determination of the stresses and strains on the normal median plane to the crack, σ_1, σ_2, ε_1 and ε_2. In particular, for $\theta = 0$, $\sigma_1 = \sigma_2$ and,

$$\sigma_3 = \frac{1-\nu}{\nu}\sigma_1 - \frac{E}{\nu}\varepsilon_1$$

In general, the plastic radius ρ will be given by the expression

$$\sqrt{\rho} = \frac{s.i.f.}{Y\sqrt{2}}\left(\frac{2\nu-1}{\nu} + \frac{E}{\nu}\frac{\varepsilon_1}{\sigma_1}\right) = \frac{s.i.f.}{2Y\sqrt{2}} E \frac{\varepsilon_1}{\sigma_1}$$

$$\rho = \rho_{max}\left(\frac{E\varepsilon_1}{2\sigma_1}\right)^2 = \frac{\rho_{max}}{m}$$

taking $\nu = \frac{1}{2}$. The parameter m may be determined experimentally be measuring the stress distribution using the photoelastic layer and the strain distribution with an embedded grating, giving a Moiré fringes pattern on a photographic plate.

Conclusion

Within the usual assumptions of linear elastic fracture mechanics, the s.i.f. associated with a crack near a nozzle, and thus the crack severity, has been found to be given by equation 9 for a number of configurations. Attention has been drawn to the fact that the same values of the s.i.f. may be associated with different shapes of plastic enclaves and thus may not necessarily correspond to a single value of the crack severity. It is hoped that present tests being undertaken in the U.S.A. [8] and in the U.K. will help to clarify this point.

References

[1.] Lamble, J. H.., 'The sandwich technique in photoelasticity'. Strain 1969, 4, 205.

[2.] Ruiz, C., 'Experimental determination of the stress distribution around notches and slits in cylindrical pressure vessels', Experimental Stress Analysis Conf., Cambridge 1970, I.Mech.E., paper 8.

[3.] Deacock, J., 'Fatigue tests on pressure vessel connections', 1st Inter. Conf. Pressure Vessel Technology, Delft, 1969, ASME/KIvI, paper II-58.

[4.] Mershon, J.L., 'PVRC research on reinforcement of openings in pressure vessels' Welding

Res. Council, Bulletin No. 77, 1962.

[5.] Chukwujekwu, S.E. and Ruiz, C., 'Experimental investigation of the plastic limit pressures of reinforced openings in cylindrical shells', Trans ASME, J.Eng. for Industry 1969, 91B, 710.

[6.] Smith, F.W. and Alavi, M.J., 'Stress intensity factors for a part-circular surface flow', 1st Inter. Conf. Pressure Vessel Technology, Delft, 1969, ASME/KIvI, paper II-62.

[7.] Boyd, G.M., 'From Griffith to C.O.D. and beyond', private communication, 1970.

[8.] Derby, R., Oak Ridge Nat. Lab., U.S.A., private communication, 1970.

Table I - General dimensions of models used

Model No	1	2	3	4	5	6	7	8	9	10	11	12	13	14
Nominal O.D. (mm)	100							77.5	100					
D/T	13	13.4			13.2			9.4	9.7	15	20	9.7	15	20
D/d	5	2			3.45			3.5	2			3		
T/t	5	2						.75	2					
r_i/T	½	½		1/3	1/9	1/3	1	1/10						
r_o/T	½	½	1/1.5		½			1/10						

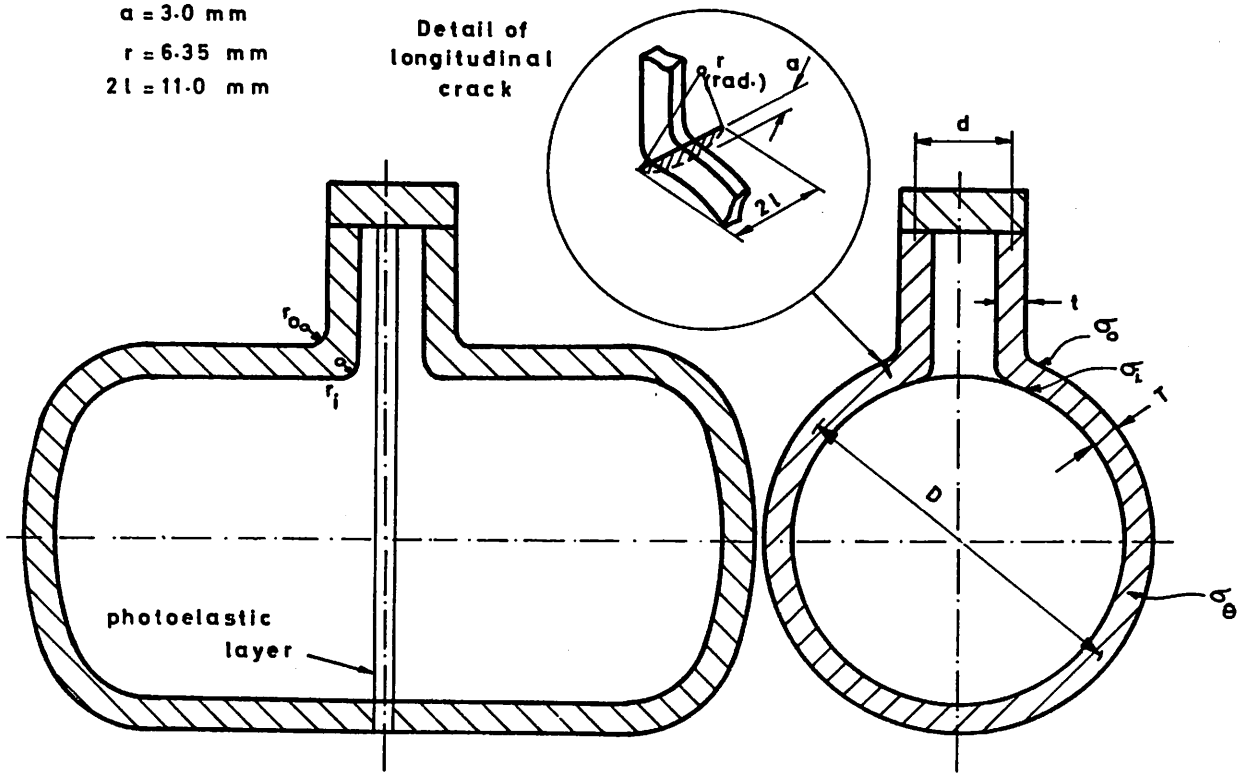

Fig. 1 General dimensions of models used.

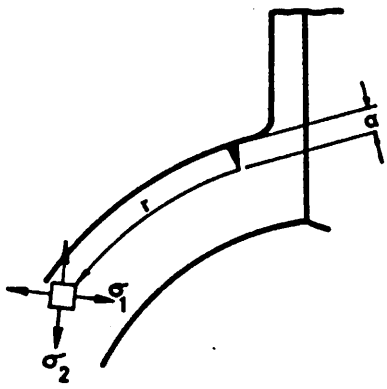

Fig. 2 Definition of stress intensification factor.

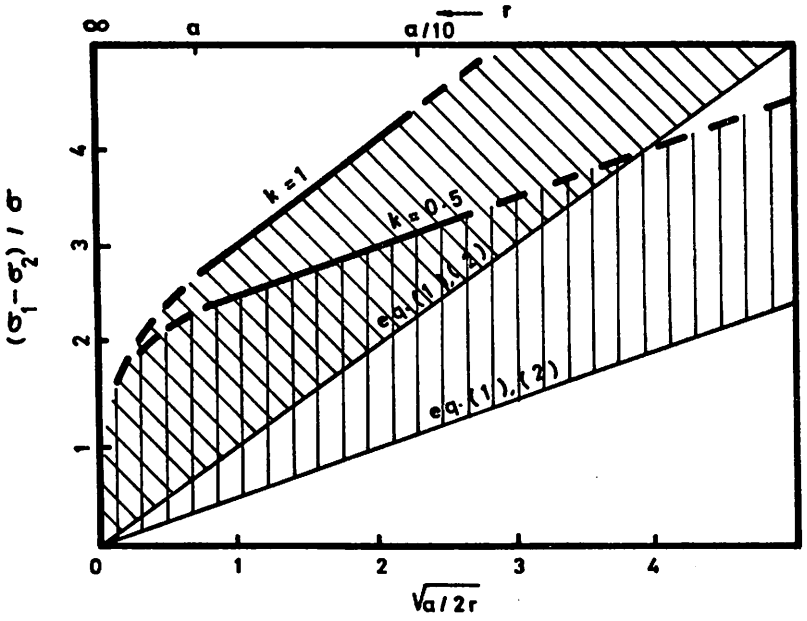

Fig. 3 Representation of $(\sigma_1 - \sigma_2)/\sigma$ against $\sqrt{a/2r}$.

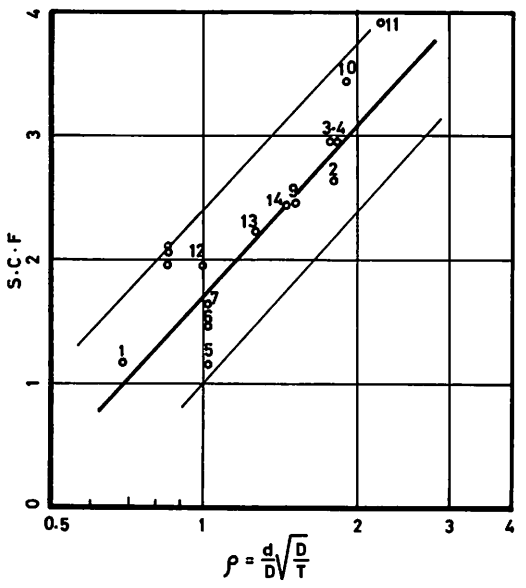

Fig. 4 Experimental values of S.C.F.

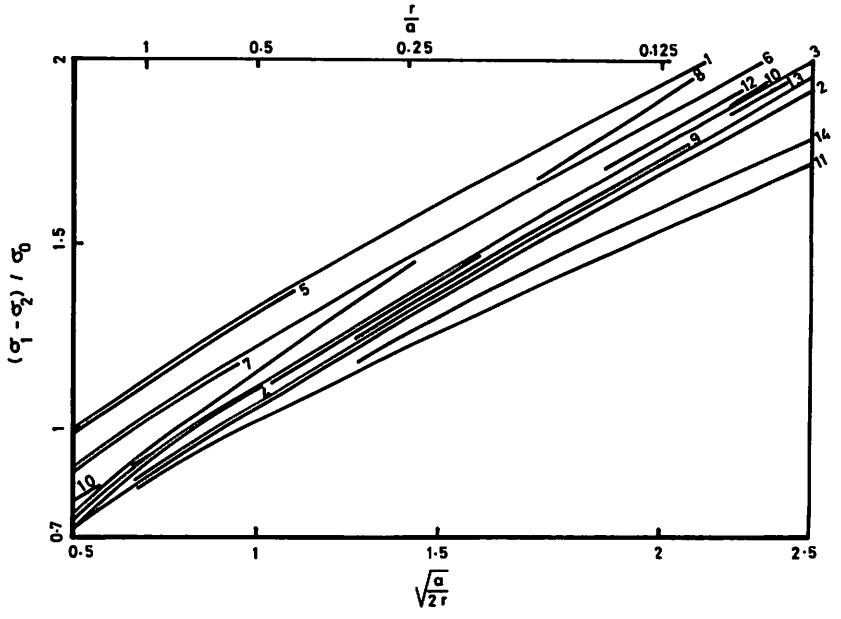

Fig. 5 Experimental values of s.i.f.

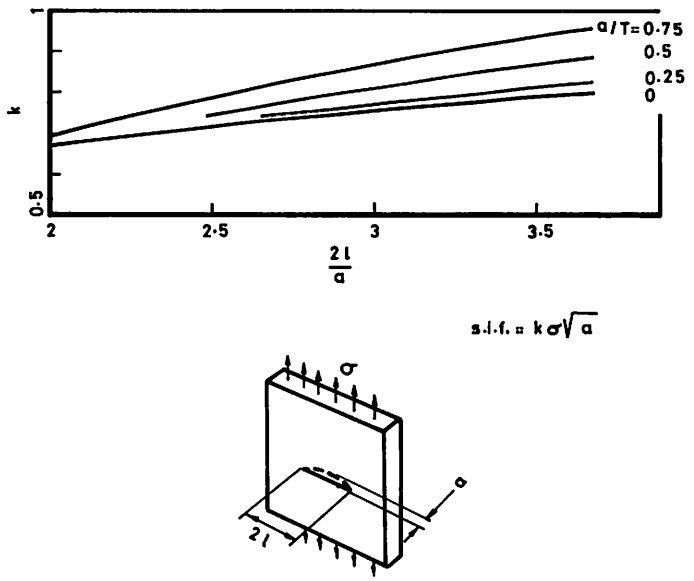

Fig. 6 Stress intensification factor for a part-circular crack in a plate loaded in its plane. (Numerical solution).

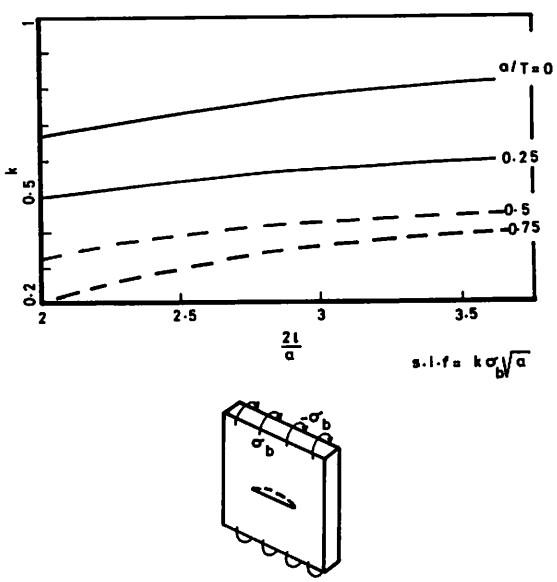

Fig. 7 Stress intensification factor for a part-circular crack in a plate loaded in bending (Approximative numerical solution).

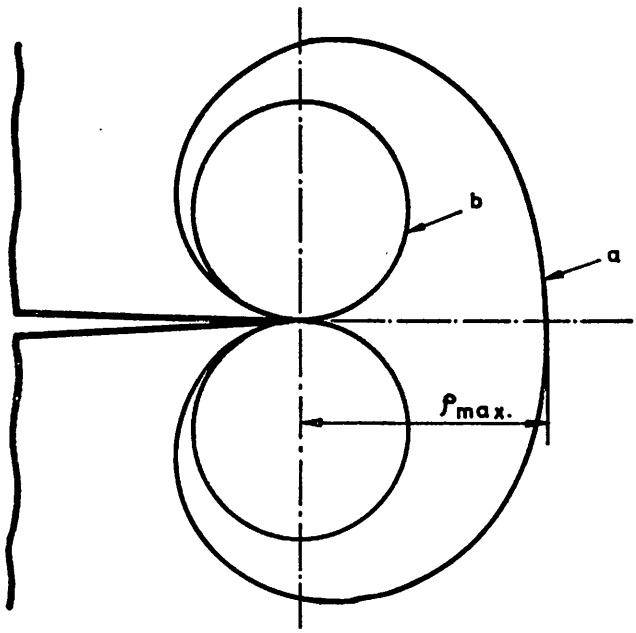

Fig. 8 Theoretical yield loci for (a) plane stress and (b) plane strain.

DISCUSSION

Q F. KERKHOF, Germany

I should like to call your attention to the "shadow-optical" method which had been developed in my institute (Institut für Festkörpermechanik, Freiburg/Br.) by Dr. Manogg. This method is based upon the simple fact that the picture of a loaded crack tip for instance in a plate is surrounded by an almost circular shadow, if the picture is unfocussed. Then the diameter of this shadow is a measure of the stress intensity factor. Did you also apply this method or do you think that it could be applied ?

A C. RUIZ, U. K.

I must express my thanks to Professor Kerkhof for pointing out to me a technique of which I only knew very vaguely and would be grateful to obtain further details. In my work I was concerned not only with the actual measure of the stress intensity but also with the way in which the crack affected the overall field. For this purpose I feel that the technique I used was particularly well suited.

C P. S. THEOCARIS, Greece

The author must be congratulated for the fine job done by using birefringent coatings and Moiré method for evaluating stress intensities at the vicinity of crack tips.
It is, however, worthwhile mentioning that both classical and experimental methods are excellent in evaluating the stress distribution around cracks but they can be used to define the stress singularity at the crack tips from which the stress intensity factor of the crack depends.
There are other experimental methods which are more effective in doing so. One of these methods will be developed later on in the presentation of my paper G 6/7.

Q A. FREDDI, Italy

In your experiments you have utilized Araldite as optically sensitive material. The behaviour of such plastic cannot be considered perfectly elastic. Is the plastic effect of small-scale type to justify the interpretation of stresses in term of linear elastic analysis ? Do you think that measurement of stresses can be performed with "freezing photoelastic technique" or the elasto-plastic behaviour and the different Poisson's number of Araldite doesn't permit in this case an elastic interpretation ?

A C. RUIZ, U. K.

In the optical layer models loading was effected entirely in the elastic field. There were thus no problems introduced by plastically induced residual stress patterns and the

Araldite and the results were of direct application to the linear elastic fracture mechanics problem. I agree that the use of the frozen stress technique can lead to difficulties if only because the actual geometry is altered. On the other hand, early results by Dixon of the National Engineering Laboratory and Fessler of Nottingham University using such technique in thick plate models have shown remarkably good agreement with rigorous theoretical solutions.